

ULTRAVIOLET LASER BEAM AND CONFOCAL MICROSCOPY

A System for Rapid Patterned Photolysis



© IMAGESOURCE

Fluorescence microscopy is generally used for the research of biology, medical sciences and other life science fields. Especially, recent advances in laser technologies and in optical engineering have made it possible to investigate the nanoscale mechanisms of physiological and molecular biological processes and thus to extend its application to pathological and clinical investigations in therapeutic sciences. Furthermore, quantitative measurements of the small molecules, ions and proteins participated into the processes in living tissues, in vivo and in vitro, its movements, and locations can be observed with these optical technologies. Among them, the confocal microscopy was firstly invented for the purpose of visualization of such small-scale observations by using proper fluorescent molecules together with laser beams. Although contrast and resolution are degraded by strong scattering of the tissue preparations in the wide field conventional fluorescence microscope, the development of the confocal microscope can overcome some of the effects of scattering, since the detector pinhole rejects fluorescence from off-focus locations. In spite of

*H. Kojima, E. Simburger,
C. Boucsein, T. Maruo,
M. Tsukada, S. Okabe,
and Ad. Aertsen*

its improvement, scanning a single section by laser beam excites, and thereby damages, the entire specimen. Furthermore, the pinhole also rejects signal photons, that are scattered on their way out of the preparation, emanating from the focal points and thus the conventional confocal microscopy is unacceptably wasteful in terms of signal photons at the deeper layer in tissue preparations. Furthermore, the undesirable effects such as phototoxicity and photobleaching could be evoked by the increased fluorescence excitation for compensating of signal-loss. Wide-field and confocal microscopy are thus techniques that are best applied to thin specimens, such as cultured preparations (for example, organotypic brain slice culture) or the most superficial cell layer in a tissue (such as acute brain slice preparations) ($<20 \mu\text{m}$).

Then, the measurements at the deeper layers in tissue preparations benefit from two-photon confocal [TPC; also referred to as two-photon excitation (TPE), or multiphoton excitation] microscopy, which allows high-resolution and high-contrast fluorescence microscopy deep in the brain even

in vivo. A large number of papers more than one thousand publications have described about the employments, developments and also reviewed this microscopy technique such as in vivo preparations since TPC had been invented [11]. In the present paper, we will follow a brief introduction of TPC and its applications to neuroscience including our newly developed photolysis (uncaging) system using an ultraviolet laser beam for the purpose of fast multipoint activation of synapses of dendrites and presynaptic neurons and neural circuits for experimental and computational neuroscience.

Principles of Two-Photon Confocal Microscopy

As each excitation even induces the risk of photodamage, such as photobleaching and phototoxicity, the application of fluorescence microscopy to living preparations is critically and inevitably limited by these photodamages. Maximizing the probability of detecting a signal photon per excitation event but minimizing photodamage is the best tuned and optimized fluorescent microscopy. In this meaning, TPC microscopy dramatically improves the detection of signal photons per excitation event compared to other techniques, especially when it takes images from deeper layers in highly scattering environments in tissues.

In the typical TPC microscopy, two photons with low-energy (usually from the same laser source such as infrared) work cooperatively to produce a higher energy transition in a fluorescent molecule and this two-photon excitation is a nonlinear process in which the absorption rate depends on the second power of the light intensity. In a well focused laser beam, the intensity of the laser beam is highest at the small focus region and drops off quadratically with distance above and below the focus. Thus fluorophores are consequently excited almost exclusively in a tiny diffraction-limited focal volume. The most fluorescence excitation occurs in a focal point region that could be around and less than $\sim 0.1 \mu\text{m}^3$, if the laser beam is focused by a high numerical aperture (NA) objective.

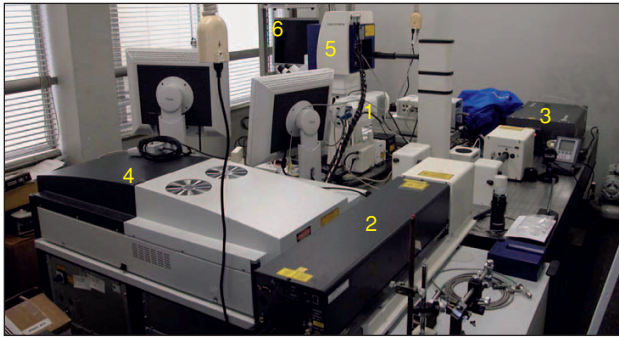
The focused laser beam scanned over the specimen in order to generate an image. Localization of excitation by this scanning produces consequently three-dimensional contrast and resolution without the necessity for spatial filters in the detection path. The excitation only in the small focal volume leads to that all fluorescence photons captured by the microscope objective constitute useful signal. When imaging in thick specimens, the signal yield per excitation event is enhanced. The properties of 2-photon excitation discussed so far are independent of scattering. The paths of the excitation photons are deflected due to inhomogeneities in the index of refraction, when excitation photons enter tissue. About a half of the incident photons are scattered every 50–200 μm depending on the condition of tissue and the wavelength of the light. The scattering of excitation light effectively reduces the light delivered to form the diffraction-limited focus and also perturbs the trajectories of fluorescence photons on their way out of the tissue.

Two-photon excitation microscopy has the following three important advantages in scattering specimens when compared to one-photon excitation: 1) Scattered excitation photons are so dilute that they cannot cause sufficient fluorescence because of the nature of nonlinear excitation. Even deep in tissue speci-

mens, under conditions where most of the incident photons are scattered, excitation is therefore still mostly limited to a small focal volume. 2) Because of reduced scattering and reduced absorption by endogenous chromophores, the excitation wavelengths such as near IR, which is used in two-photon excitation microscopy, can penetrate tissue specimens better than the visible wave-lengths of one-photon confocal microscopy. 3) All fluorescence photons (ballistic and scattered) constitute useful signal for making images if they are caught by a detector because of a fine localization of excitation source. However, in wide-field and one-photon confocal microscopy, scattered fluorescence photons are either, lost, or worse, contribute to background. This advantage of two-photon microscopy can be very important, because the majority of fluorescence photons are scattered in the typical experiments in tissue preparation.

Multipoint Photolysis with a Special Ultraviolet (UV) Laser Beam Deflector

Neurons integrate synaptic signals from many thousands of inputs. Understanding the resulting information processing at the dendritic trees and/or somata is one of the central themes in experimental and computational neuroscience at a single neuron level. Moreover, the physiological and anatomical investigation of local neural circuits in the central nervous system is also one of the most important topics for understandings of the functional mechanism of animal behaviors. In order to carry out these researches experimentally, it is generally the most popular technique to conduct electrophysiological measurements, using recording and stimulating electrodes from in vitro slice and cultured preparations, that have been developed for many years. However, these experimental techniques use conventional electrodes for direct stimulation of neural fibers and/or neurons to activate functional synapses which have synaptic contacts with other neurons, and it is almost impossible to apply and access more than three or four electrodes simultaneously to an in vitro preparation such as a slice due to less space around a preparation. Thus, three questions naturally arise from the difficulties of the conventional method of stimulation which uses the electrodes for electrophysiological experiments. Firstly, can we stimulate a small point or region such as a spine and/or synaptic active zone, or a single fiber (axon)? Second, can we mimic or reproduce experimentally and artificially the postsynaptic currents which have the same time courses and amplitudes with those observed in naturally functioning synapses? Finally, can we reproduce the complicated synaptic inputs patterns, such as in vivo preparation, to neurons of in vitro preparations? Several experimental methods have been developed to solve these questions in recent years. For example, to activate receptor ion channels, a fast agonist (or chemical compound) application by a glass θ -tube quickly driven by piezo element to a larger membrane area was developed by Colquhoun et al. [3]. This membrane patch of out-side out patch-clamp configuration excised from the membranes of neurons has involved a comparative number of receptor ion channels. More advanced technology is photolysis (uncaging) of caged compounds, such as caged glutamate and caged



1. *Photographical view of laser confocal microscopy and ultraviolet laser photolysis system with electrophysiological set-up. 1) Galvanometer based ultraviolet laser beam deflector for multipoint photolysis (DuoScan unit). 2) Unit of ultraviolet laser for ungaing connected to acousto-optical tunable filter (AOTF). 3) Unit of infrared laser for two-photon imaging (Chameleon XR, coherent, CA). 4) Control unit for confocal laser microscopy with multiargon, green HeNe, and Red HeNe laser. 5) Scanner and photomultiplier detectors for imaging with confocal and two-photon mode. 6) Set-up for electrophysiological recording with patch clamp amplifier, pulse generator, data acquisition interface, and PC.*

GABA, by ultraviolet (UV) or infrared (IR) laser beam which have been focused into diameters of less than a few μm at a focal plane of tissue preparations to activate single synaptic active zone and/or spine [1], [2], [4]–[8], [10], [12], [13].

With these focused laser beam techniques, stimulations (activations) of fine multiple point of dendrites such as active zones and spines can be carried out to study the mechanisms of synaptic sensitivities in dendrites and receptor mapping (distribution) in the membrane of neurons in combination with photolysis (uncaging) method. However, above mentioned third problem could not be overcome by this simple laser beam uncaging method due to the technical difficulties of steering laser beam rapidly and two-dimensionally in order to focus at multiple points in the same focal plane of the tissue. Recently, the introduction of TeO_2 acousto-optical crystal component into a deflector component allows ultraviolet laser beam to deflect rapidly and to perform uncaging the caged compounds such as caged glutamate at multiple points [11]. However, in this technique the UV laser beam should be transmitted through the TeO_2 acousto-optical crystal for deflection, and necessarily, the high energy UV laser source is required as a laser source due to large loss of the energy of incident laser beam. For example, they use the 1.5 W pulsed UV laser (DPSS Corp.; 50–60 ns, $\lambda = 355$ nm pulses at a 100-kHz repetition rate with average power >400 mW) which is also quite expensive and difficult to handle with for the present purpose of experiment.

To overcome this difficulty, alternatively we have developed a deflector, that steers and modulates the uncaging UV laser beam, by constructing a beam-deflector with a conventional galvanometer mirror which is controlled by special designed software. The galvanometer-deflector, which has been previously used to scan the laser beam for taking images in confocal microscopy, allows rapid access of focused laser beam to many locations in tissue. Our newly designed system could perform photolysis at over 500 locations on the tissue preparation per second, considerably faster than the older uncaging system, that was not originally designed to steer laser beams rapidly, equipped with the conventional gal-

vanometer mirrors and mechanical shutters. In the present paper, we show the basic technical characteristics (specification) of the present system, its available performance and limitations and also demonstrate the results obtained by the applications to several topics in neuroscience.

EXPERIMENTAL SYSTEM AND METHODS

General Design of the System for Photolysis

The present system for uncaging is originally designed in combination with a conventional confocal laser microscopy (LSM510 META, Carl-Zeiss MicroImaging, Jena, Germany) equipped with several visible wavelength laser sources (Ar/ML 458/477/488/514 nm, G-HeNe 543 nm 1 mW, R-HeNe 633 nm 5 mW) and an infrared Titanium:Sapphire laser (1.5 W, Repetition rate 90 MHz, pulse width <140 fs, 705–980 nm, Chameleon XR, Coherent, CA) for two-photon imaging. Ultraviolet light source for photolysis equipped in the present system is a commercial model (Enterprise II model 653, Coherent, CA) of continuous wave length argon gas laser which has 351 and 364 nm wavelength and 80 mW output power (beam diameter 0.88 mm measured at the output coupler which is 8.5 cm behind the front faceplate of the laser head assembly). The beam divergence and the waist location is 0.73 and 0.81, respectively; the long-radius output coupler acts as a weak lens to transform the output beam parameter. The values for beam divergence, waist diameter and location take into account this weak lens effect. The value for beam waist location is measured from the outside of the front faceplate of the laser head assembly. Primary wavelength(s) used for light regulation. When the ultraviolet power is set for the specified value, the visible power levels may be significantly higher than the specified values.

To introduce the ultraviolet laser beam into a microscope optics for uncaging, a single-mode delivery fiber with minimum waveguide dispersion is connected to LSM DuoScan unit (multi-purpose control unit for external laser beam manipulation, Carl-Zeiss, Jena) incorporated into the original adapter position for the mercury lamp used for standard fluorescence illumination. It was estimated that the attenuation losses of the UV laser power by equipped ultraviolet delivery fiber is not significantly large and that the laser-to-fiber coupling efficiency is high. We also introduced an optical isolator (i.e., from CVI) to decrease the feed-back from the fiber face. A commercial two dimension individually driven galvanometric scanner (scanning speed up to ~ 5 frames/s (512×512 pixels), field of view 10×10 mm² with a $1.25 \times$ objective) is used as a laser beam deflector, which is incorporated into LSM DuoScan unit to rapidly steer the ultraviolet laser beam for uncaging at a focal plane. The output power of the ultraviolet laser beam is controlled by an (shutter ON-OFF) UV-AOTF (Acousto-Optical Tunable Filter) attached to the output exit of ultraviolet laser of 653 model.

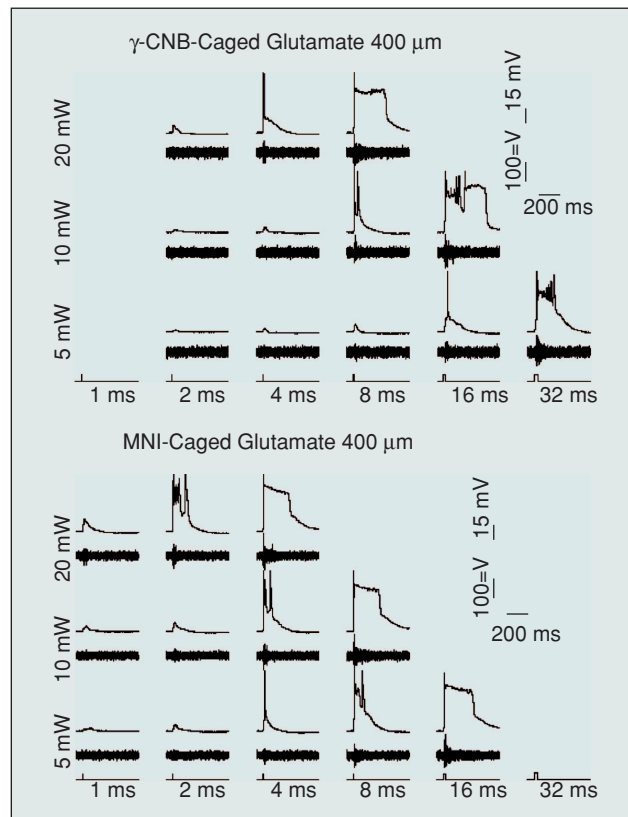
The ultraviolet uncaging beam from galvanometer is projected through focusing lens and then merged with the infrared and/or visible imaging beam using a dichroic mirror. Both beams are then directed through a $40 \times$ objective (Achromplan, 0.8 NA, Carl-Zeiss, Jena) into a single shared focal plane. In order

to ensure that the focal planes of the ultraviolet and infrared beams coincide, the images were aligned to each other, adjusting the scanfields and using collimating optics. In addition, the objective ensured high transmission in the UV and visible spectral range still providing considerable transmission in the infrared spectrum (transmission at 355 nm: ~70%, at 830 nm: ~73%). Figure 1 represents the present UV laser uncaging system with infrared and visible light laser sources for imaging, together with a set up of electrophysiology. The preliminary experiment by using the present system gives the following specification: Focal point-size of UV laser spot for uncaging (diameter) is less than $3\ \mu\text{m}$, Illumination time (uncaging park time) is adjustable from $10\ \mu\text{s}$ to $1\ \text{s}$, laser power $\sim 0.3\ \mu\text{J}/100\ \mu\text{s}$ at the focal plane of specimen, time interval between two spots is less than $1\ \text{ms}$ and $1\text{--}2\ \text{ms}$ for distance $10\text{--}40\ \mu\text{m}$ and $40\text{--}100\ \mu\text{m}$, respectively, max field view with objective (Achromplan $40\times 0.8\ \text{NA}$) is $325\times 325\ \mu\text{m}$, number of uncaging spots at present 12 on display but until 100 is possible. For electrophysiological experiment, in addition to the standard signals obtained in the conventional LSM, the following performance can be done: 1) Bleach/uncaging functionally can be triggered. 2) Time series performance combined simultaneous imaging and uncaging can be triggered. 3) Synchronous signal is set at each spot illumination to be used for recording along with the electrophysiological trace.

Comparison of γ CBN-Caged L-Glutamic Acid and MNI-Caged L-Glutamic Acid

The efficiency of two types of caged glutamic acids was tested with respect to activation efficiency of neural cells. We used the same concentration ($400\ \mu\text{M}$) of γ CBN-caged L-glutamic acid (G-7055, molecular probes, Leiden, Netherlands) and MNI-caged L-glutamic acid (Tocris) to test the efficiency of neuronal activation. The glutamate receptor channels were activated by uncaging these caged glutamates with the various energies and different illumination times of UV-laser. For this purpose, the output power of the continuous wave water-cooled argon ion laser (ENTC II 652, Coherent, Santa Clara, CA) with two emission lines at 351.1 and 363 nm could be adjusted continuously ranging from 0 to 100 mW. The laser beam with a diameter of $\sim 1\ \text{mm}$ was focused to a spot size of about $50\ \mu\text{m}$ diameter in the plane of slice tissue. The electrical measurements were carried out from acute coronal slices of somata-sensory cortex by using two sorts of recording pipettes; one is for recording of the intracellular potentials and another is for extracellular population activity from pyramidal cells. The DC resistances of the pipettes of the intracellular and population activity measurements are $3\text{--}7\ \text{M}\Omega$ and $200\text{--}600\ \text{k}\Omega$, respectively [2].

The results of testing the efficiency of two types of caged glutamates (γ CBN-caged L-glutamic acid (G-7055, Molecular Probes, Leiden, Netherlands) and MNI-caged glutamic acid (Tocris) is presented in Figure 2. Although the MNI-caged L-glutamic acid was originally developed for uncaging by 2-photon IR laser beam, it is shown from the present examination that MNI-caged glutamic acid is more effective to evoke neurons by UV-laser uncaging than γ



2. Electrophysiological experiment of comparison of physiological responses to glutamate uncaging between γ CBN-caged glutamate and MNI-caged glutamate. Axes are output power of UV laser (vertical) and illumination duration for uncaging (horizontal). Intracellular responses to single light pulses centered at soma of recorded cell are displayed in the top traces. Multiunit activity picked up by a nearby extracellular recording electrode is indicated by the bottom traces. Stimulus onset and duration are indicated by the traces in the bottom row.

CBN-caged L-glutamic acid does. Thus in our experiments, MNI-caged glutamic acid was routinely used as a caged compound for activation of glutamate receptor channels.

Rat Acute Slice Preparations and Electrophysiology

Wistar rats (12–16 day old) were anaesthetized by diethylether and rapidly decapitated. Transverse cerebellar and hippocampus slices ($270\text{--}300\ \mu\text{m}$ thickness) were cut in ice-cold ACSF (artificial-cerebra fluid solution) using a vibrating slicer (VT1000, Leica, Germany). Slices were incubated in standard ACSF bubbled with 95% O_2 and 5% CO_2 for 30–60 min at room temperature ($22\text{--}24^\circ\text{C}$) and subsequently placed at room temperature in normal ACSF containing $2.4\ \text{mM}\ \text{CaCl}_2$ and $0.6\ \text{mM}\ \text{MgCl}_2$ to reduce the background synaptic activity as Edwards et al. [5], reported. The slice preparation was moved to a chamber of which the bottom consisted of a cover slip having a thickness of $0.12\text{--}0.17\ \text{mm}$ (Matsunami Glass Inc., Ltd. Japan) and it was then immobilized on the bottom of the chamber by a grid made of a flattened platinum horseshoe-shaped frame with nylon strands glued across it with cyanoacrylate glue. The recording chamber was continuously perfused by normal ACSF at a rate of $2\ \text{ml}/\text{min}$ bubbled with 95% O_2 and 5% CO_2 . The composition of the ACSF was as follows: $127\ \text{mM}\ \text{NaCl}$, $1.6\ \text{mM}\ \text{KCl}$, $1.24\ \text{mM}\ \text{KH}_2\text{PO}_4$, $1.3\ \text{mM}\ \text{MgSO}_4$, $2.4\ \text{mM}\ \text{CaCl}_2$,

26 mM NaHCO₃, 10 mM Glucose, pH 7.4. Cell somata of Purkinje cells and pyramidal cells, which were identified by an infrared DIC (differential interference contrast) microscope, were cleaned for patch clamping. Patch pipettes were pulled from borosilicate glass tubing having a DC resistance of 4–7 MΩ. The internal solution had the following composition: 133 mM methanesulfonic acid, 7.4 mM KCl, 0.3 mM MgCl₂, Na₂ATP, 0.3 mM Na₂GTP, 10 mM Na-HEPES, pH to 7.3 with KOH (290 mOsm). All electrophysiological experiments were performed with a MultiClamp 200A (Axon Instruments, USA) patch clamp amplifier and a data acquisition interface (digidata 3221) and a software (Clampex9.0).

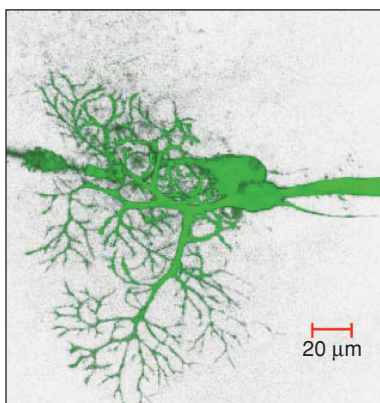
Cultured Hippocampal Cells and Electrophysiology

Hippocampal slice culture was prepared by the protocol described elsewhere [9]. The cultured cells were identified by microscopy inspection before use for experiments and transferred to a microscope chamber which is continuously perfused with Tyrode solution having following composition: 119 mM NaCl, 2.5 mM KCl, 2.0 mM CaCl₂, 2.0 mM MgCl₂, 25 mM Na-HEPES, 30 mM glucose, pH 7.4. The internal solution of patch electrodes for recording had the following composition: 140 mM CsCl, 2.5 mM EGTA, 2 mM MgCl₂, 10 mM HEPES, 2 mM TEA, 4 mM K₂ATP, pH 7.3. The electrophysiological recording was carried out by the same procedure with that mentioned in the previous section (acute slice preparations of rat and electrophysiology). Spontaneous miniature excitatory post synaptic currents (mEPSCs) were routinely recorded from the cells when the tight seal (Giga seal) between tip of the recording pipette and cell membrane of somata was formed and whole cell clamp configuration was achieved.

EXPERIMENTAL RESULTS

Responses from a Purkinje Cell by Direct Synaptic Stimulations

We carried out patch clamp electrical recording from cerebellar Purkinje cells of acute slice preparations in order to obtain the electrical responses activated by UV uncaging of caged glutamate. Caged glutamate was locally bath applied through a glass pipette (inner diameter of 5.0 ~ 10.0 μm) filled with MNI-caged L-glutamic acid of which concentration is 5 mg/mL (dissolved in 95% O₂ and 5% CO₂ bubbled ACSF). The glass pipette was accessed to the dendritic region of a Purkinje cell by visual microscope inspection and before uncaging by UV-laser beam, caged glutamate molecules were delivered at the vicinity of a Purkinje cell by a slight positive pressure applied to the back of the pipette. Figure 3 shows a three-dimensional morphological image of cerebellar Purkinje cell injected with 420 μM Calcium Green 1 (4.2 mM stock solution



3. Morphology of a Purkinje cell injected with Calcium-green 1 (420 μM) and shown by obtaining the image with two-photon confocal microscopy of mode-locked 800-nm wavelength infrared laser. The acute rat (15 day-old) slice has a 300-μm thickness, and the images were constructed from pictures taken at 1.5-μm step intervals. The cylindrical rod in the right-hand side of the picture is a recording patch pipette of voltage clamp mode.

in distilled water, hexapotassium salt, Molecular Probes) from a 300 μm thickness acute slice preparation of 2 week old rat. The morphological image was taken with a 2 photon confocal microscopy by scanning a mode-locked 800 nm infrared laser beam (Chameleon XR, coherent). After three dimensional morphological constructions of the Purkinje cell was obtained on the screen, arbitrary locations of dendrites and soma of the cell could be marked easily by mouse pointer of computer screen in order to determine the locations of the cell and to activate the glutamate receptor channels in the membrane of the dendrites and soma. UV-laser power and illumination duration for photolysis were controlled and adjusted properly for obtaining the proper electrical responses by a patch pipette applied to the soma. Patch clamp recording of voltage clamp mode from the soma was carried

out and the photolysis of caged glutamate evoked inward currents in all Purkinje cells examined. These currents were detected in the presence of tetrodotoxin (1 μM), to block voltage-gated sodium channels and cesium in the recording pipette to block voltage-gated potassium channels.

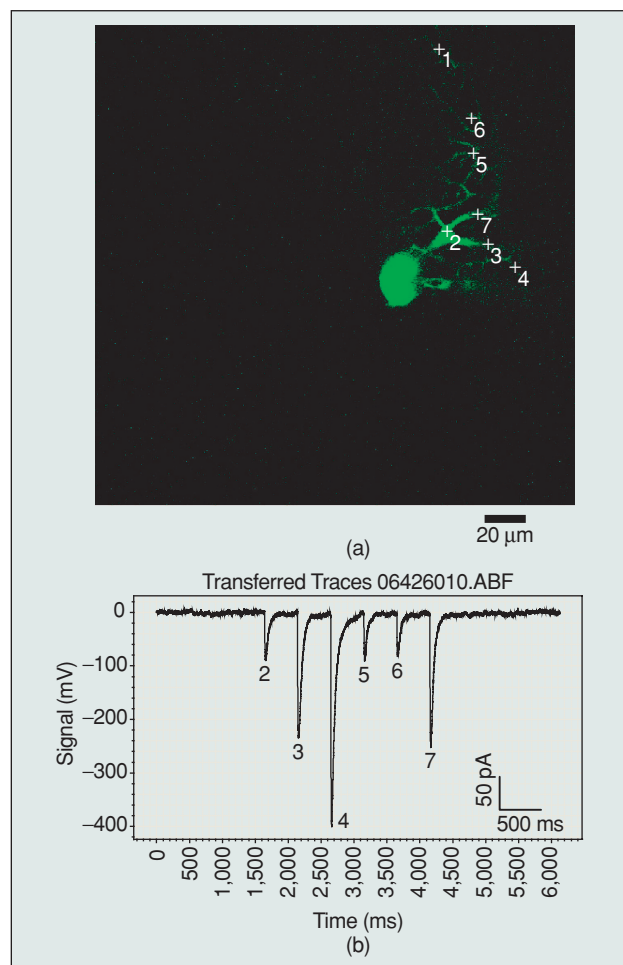
Figure 4(a) represents a typical image of a Purkinje cell with the locations (marked by crosses) at which uncaging UV-laser beam was focused (to ~3 μm) sequentially following the order of the numbers indicated (1 to 7) over dendrites and soma. The electrical responses evoked by photolysis (uncaging) of MNI-caged glutamate, which was locally applied through a glass pipette to the vicinity of the Purkinje cell, were caused by activation of glutamate receptors because they were entirely abolished by treatment with 6-cyano-7-nitroquinoxaline-2,3-dione (CNQX; 10 μM), an antagonist of α-amino-3-hydroxy-5-methyl-4-isoxazolepropionic acid (AMPA)-type glutamate receptors in combination with 2-amino-5-phosphonovaleric acid (APV; 100 μM), which blocks N-methyl-D-aspartate (NMDA)-type glutamate receptors (data not shown and the same pharmacological test was performed all other experiments in the paper). The evoked currents are presented in Figure 4(b) in which the each number of the responses corresponds to those of the Purkinje cell image in Figure 4(a). The whole cell currents were measured by a pipette accessed to the soma which was voltage clamped at a holding potential of -60 mV. The amplitudes of recorded responses are in range between -90 to -400 pA. The whole time course of evoked current traces were fitted by two-exponential functions (1st component for the rising phase and 2nd for the decay phase, respectively) and two time constants of fitted exponential function are 44.5 ± 5.8 ms and 8.2 ± 1.5 ms, respectively. These values of the evoked currents at the point 2, 3, and point 7 are almost equal each other and it is suggested that these three points are also close spot at the

dendritic location and the electrical properties and synaptic input of these three points have the equivalent effects to the soma of the Purkinje cell. However, the responses obtained by uncaging at the point 5 and 6 are smaller in amplitude and in decay time constant due to a far location from the soma which has a longer electrotonic distances compared to that of the location of 3, 4, and 7. Even if point 2 is closer location from the soma, the electrical response (amplitude) is smaller than that obtained by uncaging at the points of 3, 4, 7.

The whole cell current traces were filtered at a 5 kHz bandwidth (-3 dB), with 8-pole low-pass Bessel filter and stored into the hard disc of a PC at a sampling rate of 20 kHz. The illumination duration and power of UV-laser beam for photolysis of each location were 0.1 ms and 50%, respectively. The time interval of each location of photolysis was 500 ms. The same sequence of uncaging was repeated with sufficient time interval (0.05 Hz) to avoid the effect of the previous photolysis and each sequence showed the same amplitude and time course of evoked responses. It means that the reproducibility and reliability of the evoked inward currents are quite high by the caged glutamate activation with UV-laser beam photolysis at the dendrites of the Purkinje cell.

Activation of Granule Cells by UV-Laser Photolysis

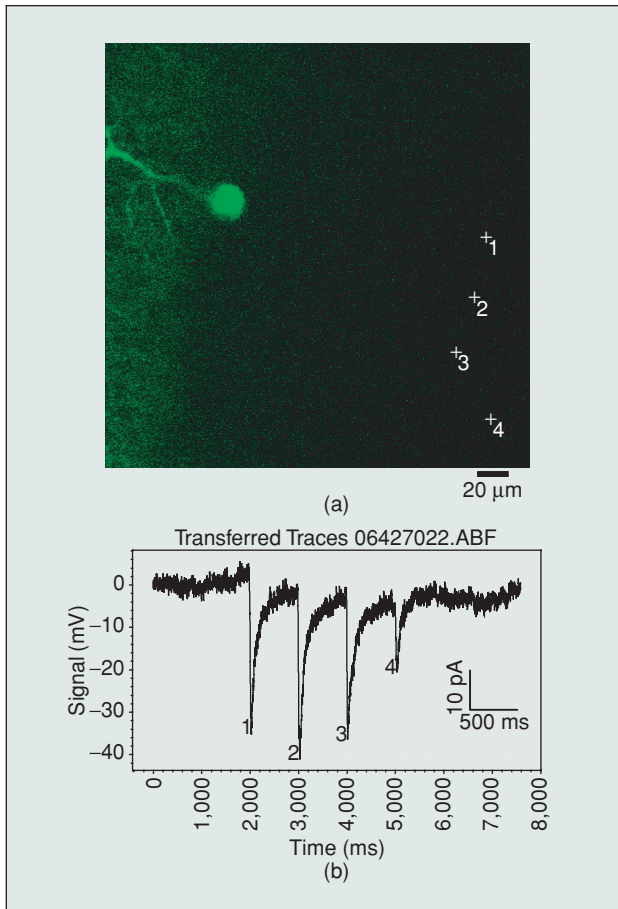
Rat Purkinje cell dendrites receive more than $\sim 150,000$ excitatory synaptic inputs through parallel fibers which are the axons of granule cells in granule cell layer and have one-to-one synaptic contact. To activate parallel fiber to Purkinje cell synapse it is necessary to stimulate directly the parallel fibers and/or granule cells by electrodes or patch pipettes placed on these structural elements. For example, the long-term depression of the synapse between parallel fiber and Purkinje cell are observed by test stimulation to parallel fibers after the conjunctive treatment of parallel fibers and climbing fibers stimulation. We stimulated each granule cell directly by UV laser uncaging of caged glutamates and recorded the synaptic responses from the soma of the Purkinje cell on which the parallel fiber of the activated granule cell has a synaptic contact. Figure 5 shows the recorded electrical responses (synaptic currents) by illuminating the crossed spots of granule cell layer of slice preparation applied with caged glutamate, and the illumination for photolysis was done by UV-laser beam of the wave length both 351 and 364 nm. The illumination time and laser power of each point were 0.5 ms and 50%, respectively and the time interval between every photolysis was 1 s. The MNI-caged glutamate molecules were locally bath applied through a glass pipette which was approached above the granule cell layer of the slice preparations. Each synaptic current is almost equal size in amplitude and time courses except the amplitude of the number 4 which is located more far away from the Purkinje cell soma (upper left of the figure). Activated synaptic currents of spot number 1, 2 and 3 have the amplitudes of around $30 \sim 40$ pA. However, the amplitude of activated synaptic current of spot number 4 is ~ 15 pA. The decay phase of activated synaptic currents is fitted by double exponential functions. The mean values of the time constant of the first and slow component of



4. Multispot stimulation by ultraviolet laser beam. (a) Two-photon image of a Purkinje cell and locations of uncaging spots by ultraviolet laser beam over the dendrites. The numbers marked by crosses is the sequential order of uncaging locations. Recording pipette is accessed to the soma of the cell for whole cell patch clamp current recording. (b) Evoked currents, by UV laser uncaging, recorded from the soma, which was patch clamped at the holding potential of -60 mV. Numbers correspond to the locations of the dendrites of the Purkinje cell image. The evoked currents were caused by activation of glutamate receptor channels with UV laser photolysis, and its amplitudes varied depending on the location of the dendrites uncaged. This variation in amplitude change was reproducible in each trial.

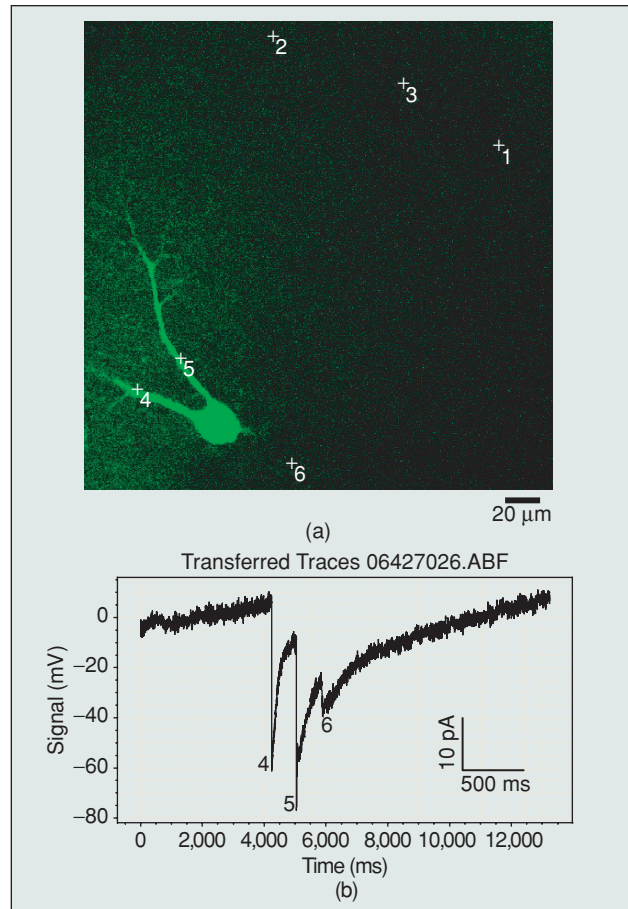
two exponential functions are 81.04 ± 11.7 ms ($n = 4$) and 395.08 ± 206.04 ms ($n = 4$), respectively.

Anatomical studies have indicated that the axonal projections from a wide area of granule cells in granule cell layer converge to a Purkinje cell through parallel fibers and the present result consistent with this anatomical observation. To verify this anatomical study more precisely by the present photolysis technique, the spots in the slice region which are supposed to have no anatomical connection with a Purkinje cell are uncaged together with three points; one point of the region of granule cells which are suggested to have a connection with a Purkinje cell and two points on the dendritic tree of the same Purkinje cell. Figure 6(a) represents the location of three points (number 1, 2, 3) which are in the molecular layer and supposed to have no anatomical connections to a Purkinje



5. (a) Two-photon image of a Purkinje cell with the location of granule cells, which is supposed to have synaptic connections with it through parallel fibers. The granule cells marked by crosses were activated by direct photolysis to its soma with UV laser beam. (b) Currents recorded from the soma of the Purkinje cell by voltage clamp mode at a holding potential of -60 mV. Evoked currents were synaptic responses by the activation of granule cells that send their axons to the dendrites of the Purkinje cell through the parallel fibers and form synapses.

cell shown at the lower-left corner of the figure. Two points of the dendrite (number 4, 5) of this Purkinje cell and one point of a location of granule cell (number 6) which has a synaptic contact with it. The corresponding number of the evoked synaptic responses are shown in Figure 6(b) and the evoked currents marked number 4 and 5 indicated larger responses (~ 60 pA) due to the direct activation of glutamate receptors in the membrane of dendritic trees and current marked number 6 showed smaller (~ 15 pA) but clear glutamate receptor response which was evoked at the synapse between the parallel fiber and the Purkinje cell, and this parallel fiber originating from the axon of the granule cell located at the position of number 6. The illumination time and power of UV laser for photolysis were 0.5 ms and 100%, respectively and the time interval between spots was 800 ms. The time course of evoked responses number 4 (71.64, 131.07 ms by two exponential fitting) and 5 (46.9, 557.9 ms by two exponential fitting) are faster than that of response number 6 because 4 and 5 are evoked by direct activation of glutamate receptors by photostimulation of dendritic trees and 6 is due to the synaptic activation through parallel fiber originating from a granule cell



6. (a) Functional connections between Purkinje cell and other regions of cerebellar slice preparation, cut sagittal. 1–3 are uncaged locations having no functional and anatomical connections to the Purkinje cell; 4 and 5 are spots on which two different branches of Purkinje cell were uncaged; 6 is location corresponding to granule cell having functional synaptic connection to Purkinje cell through a parallel fiber. Image was obtained with two-photon confocal laser microscopy with 800 nm mode-locked laser beam. (b) Inward current responses from soma of cell, voltage clamped at holding potential of -60 mV. First two responses were obtained by the activation of the glutamate receptors in the membrane of dendrites. Smaller response was due to the synaptic activation between parallel fiber and Purkinje cell.

located at the position of number 6. The same concentration (5 mg/mL) of MNI-caged glutamate molecules were locally applied through a glass pipette above the region of interest.

Synaptic Activation of Cultured Hippocampal Cells by UV-Laser Photolysis

We performed uncaging experiments by using the cultured hippocampal pyramidal cells together with whole-cell patch clamp current recording from the somata of the cells, which were injected with Alexa 568 ($40 \mu\text{M}$) and identified morphologically by the confocal laser microscopy (visible wavelength 548 HeNe laser). Figure 7(a) shows an example of cultured hippocampal pyramidal cell and a marked point (number 1) of a dendritic tree is illuminated by the UV-laser beam of wavelength 351 and 364 nm in order to activate glutamate receptor channels. The MNI caged glutamate molecules were locally applied to the vicinity of the cells by the same manner with that described in the previous section regarding cerebellar

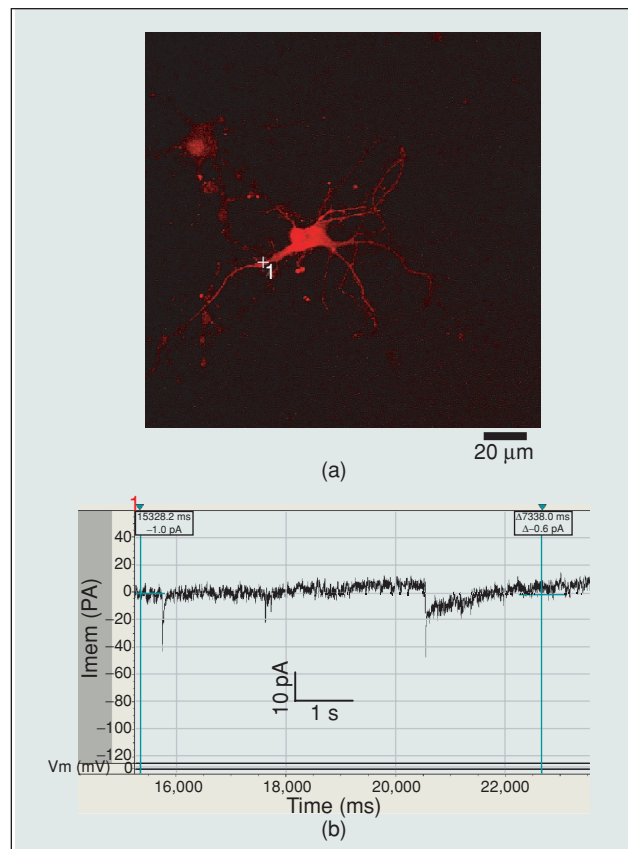
slice experiments. The cultured pyramidal cells have been incubated at 35°C for a week before use for experiments and were transferred to a recording chamber for electrical measurements. The pyramidal cell was identified from other cells by inspecting its shape morphologically, especially, of the extent of dendritic trees' shape and the area of its extension which had satellite-like and equally oriented tentacles. The recording electrodes filled with the internal solution described in method section were accessed to the somata which were voltage clamped at a holding potential of -60 mV.

The evoked current response recorded by uncaging of caged glutamate is represented in the Figure 7(b). The first two inward current traces are the spontaneous synaptic currents (excitatory postsynaptic current, EPSC) elicited at the synapses with other cells and third inward current response is the current (EPSC) mediated by glutamate receptor channels activated with UV laser photolysis. The decay phase of the currents traces was fitted by a single exponential function having the decay time constant of 21.21 ± 6.06 ms ($n = 7$) for spontaneous EPSCs and 22.66 ± 7.39 ms ($n = 4$) for uncaged EPSC-like current responses. From these results, the time constant of the 1st component of uncaged EPSCs and the main component of spontaneous EPSCs are equal values and it is suggested that these two types of EPSCs were evoked by glutamate receptor channels which were activated by the glutamate transmitters released from the presynaptic terminals and those by photolysis of MNI caged glutamate, respectively. However, the long lasting component after the 1st component of uncaged EPSC is supposed to be the inward currents flow through voltage gated Ca^{2+} channel in the vicinity of postsynaptic active zone. Other possibility of this long-lasting component was due to the persistent presence of glutamate molecules around the glutamate receptors in the membrane of dendrites and these glutamate molecules causes the desensitization of the glutamate receptor channels.

DISCUSSION AND CONCLUSION

We have developed a system for performing photolysis in arbitrary pattern in order to emulate realistic neural input activity such as in vivo preparations. The present constructed system is composed of a conventional two-photon confocal laser microscopy for imaging and a galvanometer mirror based beam deflector for steering ultraviolet laser beam for uncaging. This system is capable of patterned photolysis of caged compounds at 100 locations per ~ 200 ms with a few micron special resolutions. The ultraviolet laser beam is focused to a spot of diameter of less than $3 \mu\text{m}$ at the focal plane which makes it possible to activate a small region of the membrane such as a spine or active zone. The development of the present system could open the door to the possibility of studying how neurons integrate signals resulting from rapidly changing, complex activity conditions that until now have not been explored in vitro preparations.

The system's special resolution, which is determined by a spot size of the laser beam at a focal plane for photolysis, and the temporal resolution which is determined by the time interval between two separate locations for photolysis, are well suit-



7. (a) Confocal image of mouse cultured pyramidal cell of hippocampal area injected with dye (Alexa 568, $40 \mu\text{M}$) by a patch pipette for electrical recording. Image was taken by 548 GreenHeNe visible-wavelength laser illumination and its scanning to the cell. Number ± 1 is where UV laser photolysis was carried out. (b) Inward currents responses obtained from the soma of the pyramidal cell in (a). First two current responses were spontaneous excitatory post synaptic currents (EPSCs) mediated by synapses between the pyramidal cell and other neurons; third corresponds to an inward current evoked by glutamate receptor channels activation by UV laser photolysis 1 in (a). The MNI-caged glutamate molecules are locally bath applied to the vicinity of the cell through a glass pipette having the tip diameter of $\sim 100 \mu\text{m}$.

ed for the study of integrative mechanisms at the dendrites of a neuron receiving multi-input signals. Furthermore, the system is also applicable to investigate spatio-temporal characteristics of the dendritic integration of a single neuron which receives the complicated synaptic inputs from other neural areas. Compared with previously reported patterned activation using an acousto-optical (crystal based) deflector (AOD) which could perform photolysis at two separate locations within less than $40 \mu\text{s}$ [10], the present system is not needed to introduce a high energy power ultraviolet laser source for uncaging. It is supposed to be estimated that the higher transmission efficiency of the ultraviolet laser beam could be obtained by galvanometer mirrors than by acousto-optical crystals. For example, an ultraviolet pulse laser source which has more than 1,500 mW energy out-put power is needed for AOD in comparison with that needed for the galvanometer based deflector [11].

In addition, our system has advantages of design simplicity, possibility of using many caged compounds now available with good one-photon cross section and lower cost of uncaging laser compared with two-photon laser uncaging [8].

The present galvanometer-mirrors-based deflector has the limitation of the slower temporal resolution of uncaging between two separate locations (~1 ms) than AOD. However, this temporal resolution is the maximum value which could be achieved under the condition that the present galvanometer mirror is introduced into the system as a deflector component.

The patterned uncaging with a special resolution of sub-micron level could be achieved by the present system. Thus, it allows us to study the properties of the complicated synaptic transmission patterns, the synaptic plasticity such as a spike timing dependent plasticity (STDP) which thought to be a substantial basis of memory and learning and dendritic integration of synaptic inputs in a single neuron. Moreover, it is also capable to investigate the network level topics, for example, influence of input rate on parameters of membrane potential fluctuations, shaping of the local field potential by the synaptic input to a single cell and long-range synaptic connectivity in the slices [4], [14].

ACKNOWLEDGMENTS

We would like to thank Drs. S. Shoham (Princeton University, Princeton), I. Ilev (FDA, Washington DC) and J. Nakai (Riken, Wako) for many useful suggestions regarding the development of the present system, also thank Mr. F. Ishidate (Zeiss Tokyo) for continuous support through the work.

SUMMARY

Two photon confocal laser microscopy and imaging analysis with it are one of the central topics in the fields of biology and neuroscience. Now its applications have been extended enormously not only to the fluorescent imaging of living preparations but also to the activations of physiological processes by the introduction of laser activated photolysis of light-sensitive caged compounds. Light-sensitive 'caged' molecules provide a means of rapidly and noninvasively manipulating biochemical signals with submicron spatial resolution. Here we describe briefly a review of the recent development of multiphoton confocal laser microscopy and also a new optical system for rapid photolysis (uncaging) in arbitrary patterns by laser beams in order to emulate complex neural patterns. This system for photolysis uses a galvanometer mirrors based deflector to steer an ultraviolet laser beam rapidly and can uncage the chemical compounds at over 400 locations per second. The ultraviolet uncaging laser beam is projected into the focal plane of a two-photon microscope, allowing us to combine patterned uncaging with both imaging of neurons and electrophysiological measurements. By photolyzing caged neurotransmitter in brain slices we can generate precise, complex activity patterns for dendritic integration and also evoke a set of presynaptic neurons that give inputs to postsynaptic neurons through intact axonal projections. Our new system for photolysis with confocal microscopy allows study of the integrative properties of dendrites of a single neuron with patterned physiologically realistic input and opens new vistas in the study of signal integration and plasticity in neuronal circuit and other biological systems. Data to be obtained with our new system provides important suggestions to computational neuroscience.

REFERENCES

- [1] A.A. Bagel, J.P. Kao, C.-M. Tng, and S.M. Thompson, "Long-term potentiation of exogenous glutamate responses at single dendritic spines," *PNAS*, vol. 102, no. 40, pp. 14434–14439, 2005.
- [2] C. Boucsein, M. Nawart, S. Rotter, A. Aertsen, and D. Heck, "Controlling synaptic input pattern in vitro by dynamic photo stimulation," *J. Neurophysiol.*, vol. 94, pp. 2948–2958, Oct. 2005.
- [3] D. Colquhoun, P. Jonas, and B. Sakmann, "Action of brief pulses of glutamate on AMPA/kainite receptors in patches from different neurons of rat hippocampal slices," *J. Physiol.*, vol. 458, pp. 261–287, Dec. 1992.
- [4] I.H. Brivanlou, J.L. Dantzker, C.F. Stevens, and E.M. Callaway, "Topographic specificity of functional connections from hippocampal CA3 to CA1," *PNAS*, vol. 101, no. 8, pp. 2560–2565, 2004.
- [5] F.A. Edwards, A. Konnerth, B. Sakmann, and T. Takahashi, "A thin slice preparation for patch clamp recordings from neurons of the mammalian central nervous system," *Pflugers Arch.*, vol. 414, pp. 600–612, Sep. 1989.
- [6] S. Gasparini and J.C. Magee, "Input pattern dependent dendritic computation in hippocampal CA1 neurons," *J. Neurosci.*, vol. 26, pp. 2088–2100, Feb. 2006.
- [7] A. Losonczy and J.C. Magee, "Integrative properties of radial oblique dendrites in hippocampal CA1 pyramidal neurons," *Neuron*, vol. 50, pp. 291–307, Apr. 2006.
- [8] M. Matsuzaki, "Dendritic spine geometry is critical for AMPA receptor expression in hippocampal CA1 pyramidal neurons," *Nature Neurosci.*, vol. 4, pp. 1086–1092, Nov. 2001.
- [9] D.L. Pettit and G.J. Augustine, "Distribution of functional glutamate and GABA receptors on hippocampal pyramidal cells and interneurons," *J. Neurophysiol.*, vol. 84, no. 1, pp. 28–38, July 2000.
- [10] O. Shigeo, "Nano-scale fluorescent imaging analysis during synaptic dynamical changes," (in Japanese) *Biotechnol. J.*, vol. 11–12, pp. 744–752, 2005.
- [11] S. Shoham, D.H. O'Connor, D.V. Sarikov, and S.S.-H. Wang, "Rapid neurotransmitter uncaging in spatially defined patterns," *Nature Methods*, vol. 5, no. 11, pp. 837–842, 2005.
- [12] K. Svoboda and R. Yasuda, "Principles of two-photon excitation microscopy and its applications to neuroscience," *Neuron*, vol. 50, pp. 823–839, June 2006.
- [13] S.M. Thompson, J.P. Kao, R.H. Kramer, K.E. Poskanzer, R.A. Silver, and D. Digregorio, "Flashy science: Controlling neural function with light," *J. Neurosci.*, vol. 25, no. 45, pp. 10358–10365, 2005.
- [14] Y. Yoshimura and E.M. Callaway, "Fine-scale specificity of cortical networks depends on inhibitory cell type and connectivity," *Nature Neurosci.*, vol. 8, no. 11, pp. 1552–1559, 2005.

H. Kojima is with the Department of Intelligent Information Systems, Tamagawa University, Machida, Tokyo, Japan. *E. Simburger* is with Advanced Imaging Microscopy Division, Carl-Zeiss MicroImaging GmbH, Jena, Germany. *C. Boucsein* is with Neuobiology and Biophysics, Institute of Biology III, Albert-Ludwigs-University, Freiburg I, Br. Germany. *T. Maruo* is with the Department of Anatomy and Cell Biology, Tokyo Medical and Dental University. *M. Tsukada* is with the Department of Intelligent Information Systems, Tamagawa University, Machida, Tokyo, Japan. *S. Okabe* is with the Department of Anatomy and Cell Biology, Tokyo Medical and Dental University. *A. Aertsen* is with Neuobiology and Biophysics, Institute of Biology III, Albert-Ludwigs-University, Freiburg I, Br. Germany. E-mail: hkojima@lab.tamagawa.ac.jp. CD ■